NGAO trade study report: GLAO for Non-NGAO Instruments KAON 472 (WBS 3.1.2.1.7)

Ralf Flicker (*rflicker@keck.hawaii.edu*)
W.M. Keck Observatory, 65-1120 Mamalahoa Hwy., Kamuela, HI 96743, USA

29 March 2007

Abstract

It is shown in this report that significant gains in image quality for non-NGAO instruments may be obtained by using the NGAO laser guide star (LGS) facility together with an adaptive secondary mirror (ASM) in a ground-layer adaptive optics (GLAO) mode. Image quality gains, as reported by the full-width at half-maximum (FWHM) or encircled energy (EE), are shown range from modest to substantial depending on the observing scenario (field of view, imaging wavelength, turbulence and seeing conditions etc). All current and upcoming Keck instruments could potentially benefit significantly from GLAO improvements to poor seeing, potentially increasing the science return and efficiency manifold. For imaging, several non-NGAO Keck instruments could potentially also take advantage of the super-seeing ($0.15 - 0.3$ arc seconds) that GLAO could deliver under favorable conditions (input seeing $\sim$0.5 arc seconds), including DEIMOS and MOSFIRE.

1 Introduction

From the NGAO WBS dictionary definition of task 3.1.2.1.7 "GLAO for Non-NGAO Instruments":

> Consider the relative performance, cost, risk, and schedule of GLAO compensation using an ASM as a wide-field optical relay for non-NGAO instruments. Complete when expected performance benefit for each instrument documented.

The context which this study should be read in is that of a NGAO system that employs an adaptive secondary mirror (ASM) for ground-layer turbulence correction. There may be additional deformable mirrors on the NGAO bench or MOAO units inside NGAO specific instruments, but the ASM would be the only high-bandwidth deformable surface that is common to non-NGAO instruments, and could potentially be put to good use together with the existing NGAO LGS bouquet in order to improve image quality also for non-NGAO instruments. Implementing GLAO for non-NGAO instruments requires a WFS facility with a wide field of regard for controlling the ASM, which could be implemented in two ways:

1. Append a LGS WFS module for each non-NGAO science instrument that would be used in GLAO mode, or
2. Provided that the NGAO optical relay has a wide enough technical field of view, its WFS could potentially be reused for implementing GLAO for non-NGAO instruments. There is no obvious technical solution for how to split off the WFS light for NGAO in this mode of operation.

This study does not investigate in detail the technical challenges that either of these two options raise, but concentrates instead on the potential performance benefits of having this GLAO capability, however it might be implemented.

1.1 Benefits of GLAO

Generally, GLAO provides a relatively modest image quality enhancement most practically measured in terms of full-width at half-maximum (FWHM) or encircled energy rather than Strehl ratio. The main benefits of having this seeing-enhancement capability are:

- For imaging, the improvement in image quality, quantified e.g. by its FWHM, implies sharper and higher-resolution images.
- The improvement in encircled energy (EE) implies either higher SNR for a given exposure time, or shorter exposure times at a given SNR – both for imaging and spectroscopy (more light through the slit).
- Bad seeing nights that would otherwise be considered unusable for a certain instrument could potentially be restored to science grade observing by GLAO improvements to the seeing.

The expected performance gains is the first part of what is investigated in this report, and secondly we try to assess which currently existing and planned non-NGAO instruments could benefit from this technology. In order to be of use for many different instruments, it is one of the basic assumptions of GLAO that it is engineered to produce a large sky coverage, so that it can be applied "most of the time." For the purposes of this trade study, we shall take that to mean roughly ∼50% sky coverage at 30 degrees galactic latitude (KAON470, R. Clare[2]).

1.2 Technical challenges

Although this report does not pursue a detailed investigation of the technical challenges involved in implementing GLAO on Keck, here is a short list of some of them as a brief overview:

- The J-band low-order NGS WFS will suffer sensitivity losses in GLAO mode due to the much lesser degree of partial high-order AO correction, assuming that the LOWFS pixel sizes are optimized for NGAO levels of partial correction.
- An actuated M2 that is not conjugated to the telescope pupil plane may introduce distortions and plate scale changes over large fields of view (could potentially make the ASM closer to the pupil).
- Depending on which WFS implementation is chosen, there may be differential rotation between the ASM and the WFS module. This implies a further complication to the already complex wavefront reconstruction algorithms, that will require another level of sophistication to deal with differential rotation between the AO components.
- Any WFS implementation will have some negative consequences for the science beam. Using pick-off arms for LGS/NGS will result in vignetting of the science instrument field of view, while using dichroic beam-splitters would instead reduce throughput, increase emissivity and prevent science observations at sodium (LGS) and/or J-band (NGS) wavelengths.
- If NGAO WFSs are reused, GLAO implementation requires that NGAO is engineered to pass a fairly wide technical field of view (up to 5 arc minutes square would be good).

1.3 GLAO parameters

As will be seen from the simulation results to be presented in Sect. 4, the success of a ground-layer adaptive optics scheme is chiefly sensitive to, in order of significance:

- the relative prominence of ground-layer turbulence
- NGS tip/tilt correction fidelity, which in turn is a function of:
  - field of view
  - NGS brightness
  - number of NGSs
  - sky coverage

In addition, like any AO system GLAO is of course steeply sensitive to the imaging wavelength, with performance in the NIR being much better than in the visible. The first bullet of the list above implies that there is a strong C_n^2 profile dependency, and the the second bullet leads up to the facts that employing NGSs makes GLAO ultimately a sky coverage issue. All three of field size, NGS brightness and number of available NGS couple into the resulting

instrument	telescope	location	field(s) of view	wavelengths (μm)	pixel size(s)	comment
NIRC2	K2	Nasmyth	$40'' \times 40''$	0.9–5	small	NGAO?
ESI	K2	Cass.	$8' \times 2'$, $2' \times 3.5'$	0.4–1.1	0.15	
DEIMOS	K2	Nasmyth	$16' \times 5'$	0.4–1	0.12	
OSIRIS	K2	Nasmyth	$1' \times 1'$, $20'' \times 20''$	1–2.3	0.02–0.1	NGAO?
NIRSPEC	K2	Nasmyth	$46'' \times 46''$	0.96–5.5	0.14, 0.19	NGAO?
HIRES	K1	Nasmyth	$45'' \times 45''$	0.3–1	small	
LRIS	K1	Cass.	$6' \times 8'$	0.3–1.1	0.15, 0.21 (0.13)	image?
MOSFIRE	K1	Cass.	$6' \times 6'$	0.9–2.5	0.18	2009
NIRES	K1	bent Cass.	$2' \times 2'$	0.8-2.4	0.12	2007

Table 1: Current and future instruments on Keck I and Keck II.

sky coverage. It is assumed here to be part of the GLAO paradigm that sky coverage must be comparatively large, say e.g. better than 50% at all times.

In order to cover the range of possibilities in a limited set of simulations, a handful of observing scenarios were selected that represent the spread, without attempting to fill in the parameter space in detail. The idea of GLAO is that much of the time, most of the turbulence is concentrated to a relatively thin layer close to the ground (i.e. the altitude of the telescope). Only correcting the ground layer will not produce performance levels close to those envisioned for narrow-field tomography AO systems (such as NGAO itself), but the modest image quality improvement offered by GLAO could be obtained over a much larger field of view, and would not be dependent upon having a large number of densely overlapping reference beacons. Having overlapping beacons is important for doing atmospheric tomography, but for GLAO one may omit tomography and simply average the measurements from all beacons. Averaging the LGS WFS measurements has the effect of reconstructing chiefly the ground-layer turbulence, since this portion of the atmosphere is common to all LGS and will be amplified by the averaging process. Upper atmosphere turbulence on the other hand de-correlates quickly when the beams are widely separated, and will be attenuated by the averaging. It can be shown that tomographic methods, while severely crippled by the poor overlap of the LGS beams, can still improve performance somewhat in preferential directions (i.e. the LGS), at the expense of creating a more uneven and unpredictable image quality over the field of view. It was generally suggested in previous studies that astronomers were less interested in this than in having a uniform image quality over the field of view, so most GLAO studies to date have applied the simple averaging method.

2 Keck instruments

Table 1 lists the non-NGAO instruments that are currently foreseen to be available on the Keck telescopes by the time NGAO goes on the sky. Since it is not clear which telescope NGAO will go on, both Keck I and Keck II instrumentation listings are given. One regime of GLAO operation, that of poor seeing conditions ($> 1''$) which is improved to sub-arc-second image quality, would ostensibly lend itself to application by any existing instrument. The other regime, where already good seeing is enhanced to the $0.15'' - 0.3''$ regime, which we might call "super-seeing," places new requirements on the optical image quality of the instruments, focal plane plate scales and slit widths, if the image quality improvement offered by GLAO is to be taken advantage of in full.

Some general remarks. It may be argued that the most appealing application of GLAO would be to wide-field instruments, such as DEIMOS, LRIS, ESI and MOSFIRE, since they provide observing modes that will not be offered by NGAO. While current narrow-field instruments such as NIRC2, OSIRIS, NIRSPEC and HIRES could still benefit from seeing-enhancements, with NGAO in place it may be the case that much of their work is taken over by NGAO instrumentation, which takes advantage of the tomography and high-Strehl capabilities of NGAO (or it may be that some of these instruments are transformed into NGAO instruments, whereby we do not need to consider them for GLAO in any case). Also it should be noted that even if some instruments may be unable to take advantage of the enhanced resolution offered by super-seeing, they all benefit in terms of shorter exposure times and greater sensitivity to faint objects. With this in mind, here is a partial list of instrument specifics that might have a bearing on the instrument being used in GLAO super-seeing:

- LRIS – The red and blue channels currently have pixel sizes of 0.21 and 0.15 arcsec/pix. Adopting 2 pixels

(somewhat arbitrarily) as the desired spectral FWHM (Nyquist sampled) LRIS-red would be the most limited, unable to take advantage of seeing better than 0.4″. With the upcoming LRIS-red upgrade to a 4k×4x detector, the pixel size will be 0.13 arcsec/pix. There are concerns that LRIS in very good seeing may be limited by internal optical aberrations (possibly up to 0.4″). The instrument metrics (Keck intranet, seeing histograms from MIRA FWHM measurements using the instrument science detector) seem to support this claim, but a thorough characterization of the problem has not been done.

- ESI – $2' \times 8'$ full field in imaging mode or $2.1' \times 3.5'$ arcmin for 93×154 mm filters, with 0.15 arcsec/pix. Slit widths down to 0.3″ in Echellette mode. Imaging and Echellette mode potential candidates for GLAO at the upper end of the wavelength range (1μm).
- DEIMOS – 0.12 arcsec/pix means that DEIMOS could push angular resolution downward a fair bit in GLAO super-seeing. The full field of $16' \times 5'$ might make it hard to pick/position NGS/LGS at the edges of the field in order to avoid vignetting. This might suggest a dichroic WFS solution and a smaller LGS asterism, with GLAO performance falling off gracefully outside of the LGS asterism.
- NIRES – 1k×1k slit viewer with $2' \times 2'$ field of view and 0.12 arcsec/pix makes it viable for use with small-wide-field GLAO image enhancement.
- MOSFIRE – Has by design image quality better than $< 0.2''$ over 0.9–2.5 μm, and 0.18 arcsec/pix in imaging mode over $6' \times 6'$ field of view. As for DEIMOS, the field size of MOSFIRE may be too large for the LGS asterism to be placed around the edges of the image FoV. The GLAO performance will still be quite uniform over the field of view even if the asterism is only e.g. $4' \times 4'$, but unless the LGS are then folded to NGAO by dichroic beam-splitters, MOSFIRE might see significant vignetting from the LGS pick-off arms.

Apart from LRIS, whose internal optical aberrations are yet to be quantified, it may be possible to remove or at least reduce static instrument errors in non-NGAO instruments in general, by focal plane image sharpening calibrations using the ASM to correct static internal aberrations.

3 Numerical simulations of GLAO

GLAO was implemented in a numerical simulation by a non-tomographic wavefront reconstruction method, wherein the measurements coming from multiple LGSs are simply averaged. This method makes no assumptions about the distribution of atmospheric turbulence, and is therefore sub-optimal with respect to one that does, but it is therefore also insensitive to mistakes in those assumptions. Numerical results were produced with the AO simulation code YAO (Yorick Adaptive Optics: `http://www.maumae.net/yao/`) authored by François Rigaut (Gemini Observatory). A number of observing scenarios are described in the next section. The modeling of the GLAO system assumed the following basic system parameters, which did not vary between the different simulation scenarios:

- 33×33 single deformable mirror (the ASM), in a Fried geometry. This is presumably not the actuator geometry of a real ASM, but the exact geometry is unlikely to have a major impact on the performance of the system. Even the actuator density (the "order" of the AO system) is suggested by several to be a very weak driver for GLAO performance, with a factor of 2 in either direction making little difference.
- 32×32 sub-aperture Shack-Hartmann WFS. This is probably lower order then the actual NGAO system, whose base line is 48×48, but the dimension was chosen for congruence with the DM in order to simplify simulations. It has only a small impact on the noise in the LGS WFS, which in this study is shown not to be a driving factor for GLAO performance.
- 5-LGS (CW) asterism (quincunx), projected at 90 km altitude, sodium layer thickness 10 km
- LGS WFS system running at 1kHz frame rate, 1 additional frame delay (i.e. total latency = 2 ms)
- J-band tip/tilt NGS operating at 500Hz frame rate, no additional latency
- Second-order effects included:
  - Static segment aberrations (see WBS 3.1.1.1.3)

  - Dynamic segment aberrations (30 Hz vibrations – see WBS 3.1.1.1.2)
  - LGS spot elongation
  - LGS uplink tip/tilt control
  - LGS centroid gain optimization
  - Rayleigh back scattering (the fratricide effect)
  - 10% DM hysteresis
- Effects NOT included in this study: wind shake, misregistration, non-common path aberrations, LGS focus drifts and sodium layer fluctuations, more...

The numerical simulation is of the Monte Carlo type, where random phase screens at various altitudes translate across the telescope with different speeds, assuming the Taylor hypothesis of frozen flow. The propagation through turbulence is computed geometrically, although the SH WFS are modeled with physical optics. Scintillation may be an effect at the worst seeing and the shortest wavelength, but in that regime the residual GLAO wavefront error is around 1 μm RMS anyway, rendering scintillation uninteresting at best. 20000 frames were simulated and long-exposure PSF computed, corresponding to 20 seconds of real time exposure.

3.1 Observing scenarios

The principal parameters and the selected values that characterize an observing scenario in this study are:

- imaging wavelengths: 0.55–2.19 μm via the bands V, R, I, z, J, H, K (monochromatic narrow-band)
- field of view (LGS asterism size): $2' \times 2'$ or $5' \times 5'$
- number of NGS: 1 (central) or 4 (plus "+" asterism at same distances as LGS FoV)
- C_n^2 profile: CN–M3 (47% in ground-layer) or 13–N (67% in ground-layer) (see Fig. 1)
- seeing (r_0): $0.57''$ (18.0 cm), $1.0''$ (10.1 cm) and $1.57''$ (6.6 cm)

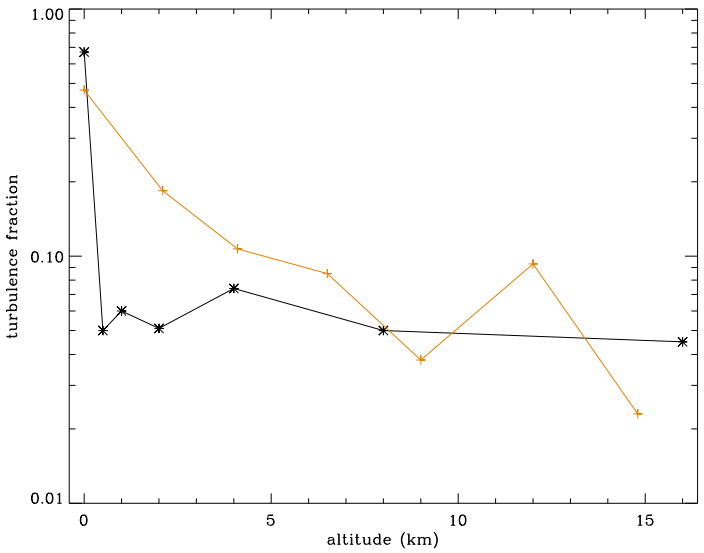

Figure 1: Turbulence profiles: 13–N (asterisks + black line), CN–M3 (pluses + orange line).

Every simulation run was evaluated at a range of science wavelengths simultaneously, so as to save us the worry of which particular band to choose. The wavelengths range from 0.55–2.19 μm, specified at the photometric bands V, R, I, z, J, H and K. Three seeing conditions were evaluated, good ($0.57''$), slightly-worse-than-typical ($1.0''$) and quite bad ($1.57''$). The field of view, number of NGS and the C_n^2 profile have only two options each, which may be

combined together differently to create a particular scenario. For such a proto-scenario, appropriate NGS brightnesses were chosen to produce the final observing and simulation scenario. While the NGS brightness could have been treated as a free parameter in order to construct unique scenarios, it must be remembered that there is a deeply embedded sky coverage issue driving these parameter choices in different directions. Increasing the required number of NGS implies smaller sky coverage; increasing the field size implies larger sky coverage; increasing the brightnesses of the NGS again implies smaller sky coverage. It was a choice made when establishing these scenarios that NGS brightnesses were to be adjusted for a given scenario in the direction of keeping the resulting sky coverage close to a nominal value. Based on WBS 3.1.2.2.10 ("Number and Type of LOWFS" KAON 470) and R. Clare (private communication), NGS brightnesses for the $2' \times 2'$ LGS FoV was constructed to represent roughly $\sim 50\%$ sky coverage, which resulted in NGS J-magnitudes of 15 for the single NGS and 17 for 4 NGS. For the larger field size scenario ($5' \times 5'$), these magnitudes were simply adjusted up by one magnitude to 14 and 16 respectively (values summarized in table 2).

LGS FoV	# NGS	NGS J mag.
$2' \times 2'$	1	15
$2' \times 2'$	4	17
$5' \times 5'$	1	14
$5' \times 5'$	4	16

Table 2: NGS brightnesses.

In preparing to run numerical AO simulations for the GLAO study, two regimes of the AO system configuration parameter space were identified as uninteresting for a 20 hr trade study on this topic. On the one hand, cases where the field of view approaches that of the largest FoV considered for NGAO in tomographic mode ($\sim 1'$) are not considered here, since in those cases it would benefit the observer to make use of NGAO instrumentation instead, so as to take advantage of MCAO or MOAO performance gains. At the other end of the spectrum are "extremely large" (in the world of AO) fields of view (larger than, say, $\sim 7'$), where, on the one hand, the performance of GLAO becomes so marginal as to be hard to measure, and secondly it seems unlikely that NGAO is going to be able to pass such a large technical field for the added-value purpose of implementing GLAO. Hence, two potentially realistic observation scenarios were here represented by LGS asterism sizes of $2' \times 2'$ and $5' \times 5'$, both with an additional guard ring of evaluation points outside of the LGS FoV, in order to assess the fall-off of GLAO performance outside of the LGS FoV. This intermediate region can be thought of as a region in parameter space where the LGS FoV is too large to make tomography really tractable, but not so large as to render the image quality gain uninteresting. Upon reviewing the results, one may therefore keep in mind that they would be better for a smaller field of view, and worse for a larger.

4 Numerical results

Figures 2-6 show the results of the numerical GLAO simulations, as expressed in four different metrics: FWHM, Strehl ratio, diameter of 50% encircled energy, and fractional encircled energy at a diameter of 225 milli-arcseconds. This metric was included for comparison with previous GLAO studies undertaken by other projects (Gemini GLAO FSR, VLT MUSE), which specified the ensquared energy within a $0.2''$ pixel as a bench mark of interest for certain instruments.

Figure 2 is an example of the output for a given observing scenario, which shows all the available information for this scenario. The solid black line with diamond plotting symbols in all four graphs are the seeing limited reference values. In the first panel of FWHM, a function has been fitted to the observed seeing as a function of wavelength (dashed orange line) based on the Kolmogorov assumptions that *seeing* $\propto \lambda / r_0$ and $r_0 \propto \lambda^{6/5}$. The coefficient of the power-law fit gives an estimation of the seeing. This turns out to be one of the most cumbersome – but possibly most pertinent – ways of measuring the effective r_0 in the simulation. The trouble with Monte Carlo simulations is that, because it relies on randomness, you don't always get exactly what you tell it to produce. As an entirely typical example, you might tell the simulation to effectuate an r_0 of 17 cm, measure it from the phase screens in the loop (with an "r_0-meter") to be approximately 19 cm, and then measure the FWHM of the PSF and calculate

an r_0 of 18 cm.[1] The latter value is what was adopted and which is reported in this text when r_0 values are cited. The green pluses plot the performance at different field evaluation points within the given FoV, and the black solid line with pluses is the weighted field average based on these evaluation points. The red pluses show the performance on a guard-ring of extra evaluation points outside of the LGS FoV. For the $2' \times 2'$ LGS FoV, this extended FoV is $3' \times 3'$; for the $5' \times 5'$ LGS FoV the extended FoV was $7.5' \times 7.5'$. This was done in order to investigate how quickly performance drops off outside of the LGS/NGS FoV.

Since there are a total of 24 observing scenarios, I could show you 23 more plots like Fig. 2. In the interest of everybody's sanity, the next three figures only plot the field-averaged metrics as calculated from the green pluses in Fig. 2 (anybody interested in what the red pluses are doing, contact the author). Figures 3-5 hence combine all the observing scenarios into one graph, one for each seeing condition. The various scenarios are coded as follows:

1. Color – turbulence profile: CNM3 (orange), 13N (red)
2. Line-style – LGS field size: $2'$ (solid), $5'$ (dashed)
3. Symbol – number of NGS: 1 (pluses), 4 (triangles)

This coding is retained throughout Figs. 3-6. A caveat needs to be pointed out for Fig. 5 and the graphs in Fig. 6 pertaining to the poorest seeing condition ($D/r_0 = 152$). By an under-dimensioned choice of simulation grid size and plate scales, the worst seeing condition caused some light to be scattered outside of the simulation grid (but wrapped around by the Fourier transform) at the shortest wavelengths. This affected the measurements of FWHM and EE of the seeing-limited images between V-I band. In order to compensate for this, a Gaussian fitting process was employed in order to reconstruct the parameters and recover the metrics. This was only partly successful, and the conspicuous looking nonlinearities close to 0.5 μm are remaining artifacts from this effect which could not be completely removed. It is a significant aberrant effect at the V, R and I data points for $D/r_0 = 152$, leading to an overestimation of the performance gain by as much as 50%. This is, however, in the region of very low performance gains (~ 1), and the error does not alter the interpretation of the results nor the general conclusions of this report.

Finally Fig. 6 focuses on two of the metrics, FWHM and 50% EE diameter, and plots the performance *gain*, as defined loosely here by the seeing-limited value divided by the GLAO value. A gain of one implies no GLAO correction (but it did not make things worse either). It is seen from all plots that, when NGS brightness are adjusted for sky coverage, there is little difference in performance differences between the various narrow/wide LGS field and 1/4 NGS combinations.

5 Recommendations

From the performance estimates it is clear that there are potential benefits, ranging from modest to significant, to non-NGAO instruments from a GLAO implementation. If a GLAO system for Keck was pursued (independently of NGAO), assuming the existence of an ASM and at least 4 LGS, the next most important technical study should investigate the most efficient WFS implementation, and look at technical solutions that offer the best cost/capability trade. At one extreme, if the NGAO WFS could be reused, GLAO could be made available to all instruments on that particular telescope. At the other extreme, new WFS modules could be built exclusively for each non-NGAO instrument that wanted to use GLAO. Somewhere in between, it might be possible to build a single GLAO WFS module that could make GLAO available to all instruments at a given focus, e.g. all Nasmyth instruments or all Cassegrain instruments.

6 Other GLAO studies

Implementing GLAO on Keck using an adaptive secondary mirror is similar in scope to several other GLAO project studies undertaken by, e.g.. the Gemini Observatory, SOAR, ESO (VLT/MUSE), TMT and GMT. We find in the current study exactly as in another recent GLAO investigation that: "These performance gains are relatively insensitive to a number of trades including the exact field of view of a wide field GLAO system, the conjugate altitude and actuator density of the deformable mirror, and the number and configuration of the guide stars."[1] Comparing

[1] In this particular case, the slight variation in effective seeing between observing scenarios that should have the same input seeing arose from the two different field sizes that were simulated. While the phase screens were pre-computed and identical for all scenarios, the different field sizes caused slightly different subsets of the screens to be used (to accommodate for larger or smaller viewing angles).

the performance gains estimated in the current study, those reported in [1] and the Gemini GLAO FSR[3], we find further support that GLAO performance is a relatively weak function of actuator density, and that we were justified in modeling the Keck ASM simply and solely as a 32×32 square actuator array, even though this model may be (significantly) different from the real ASM. All these findings are concordant with earlier analytical studies of GLAO, including [4].

References

[1] D. R. Andersen, J. Stoesz, S. Morris, M. Lloyd-Hart, D. Crampton, T. Butterley, B. Ellerbroek, L. Jolissaint, N. M. Milton, R. Myers, K. Szeto, A. Tokovinin, J.-P. Véran, and R. Wilson. Performance Modeling of a Wide-Field Ground-Layer Adaptive Optics System. *Publ. Astr. Soc. Pac.*, 118:1574–1590, November 2006.

[2] Richard Clare. Keck NGAO sky coverage modeling. Technical report, W.M. Keck Observatory, 2007. KAON 470.

[3] Gemini Ground Layer Adaptive Optics Fesibility Study Report. Internal report GLAO-PRO-001, Gemini Observatory, 23 February 2005.

[4] A. Tokovinin. Seeing Improvement with Ground-Layer Adaptive Optics. *Publ. Astr. Soc. Pac.*, 116:941–951, October 2004.

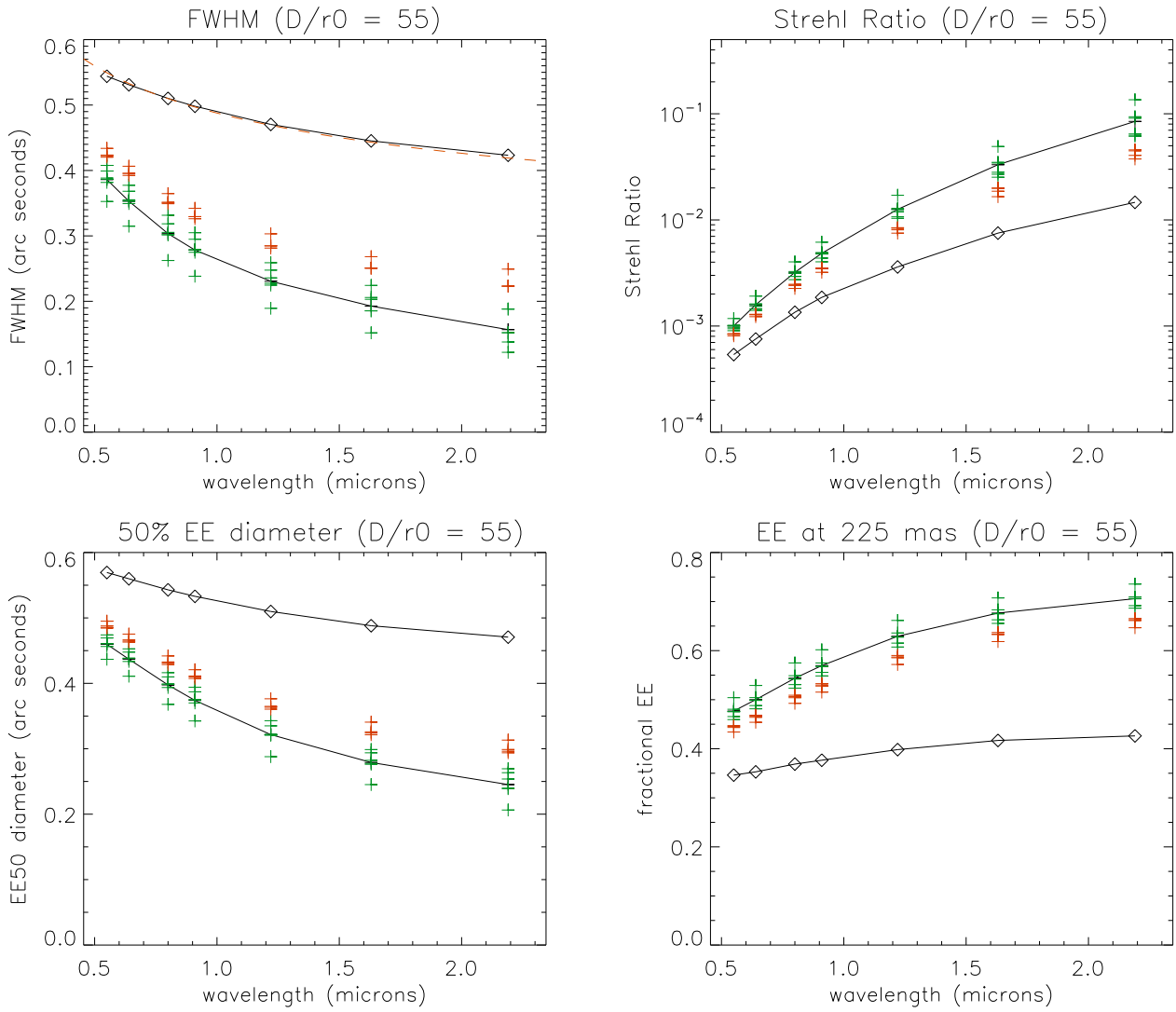

Figure 2: Simulation results for one specific observing scenario: $2' \times 2'$ LGS FoV, 1 NGS, CN–M3 turbulence profile and $0.57''$ seeing. In all graphs, the seeing limited reference is plotted in solid black line with diamond symbols. Over-plotted in the orange dashed line is a power-law curve fit that determines the seeing for this simulation to $0.57''$. Green pluses: field evaluation points within the LGS FoV; black solid line with pluses: weighted field average based on green pluses; red pluses: evaluation points outside of the LGS FoV.

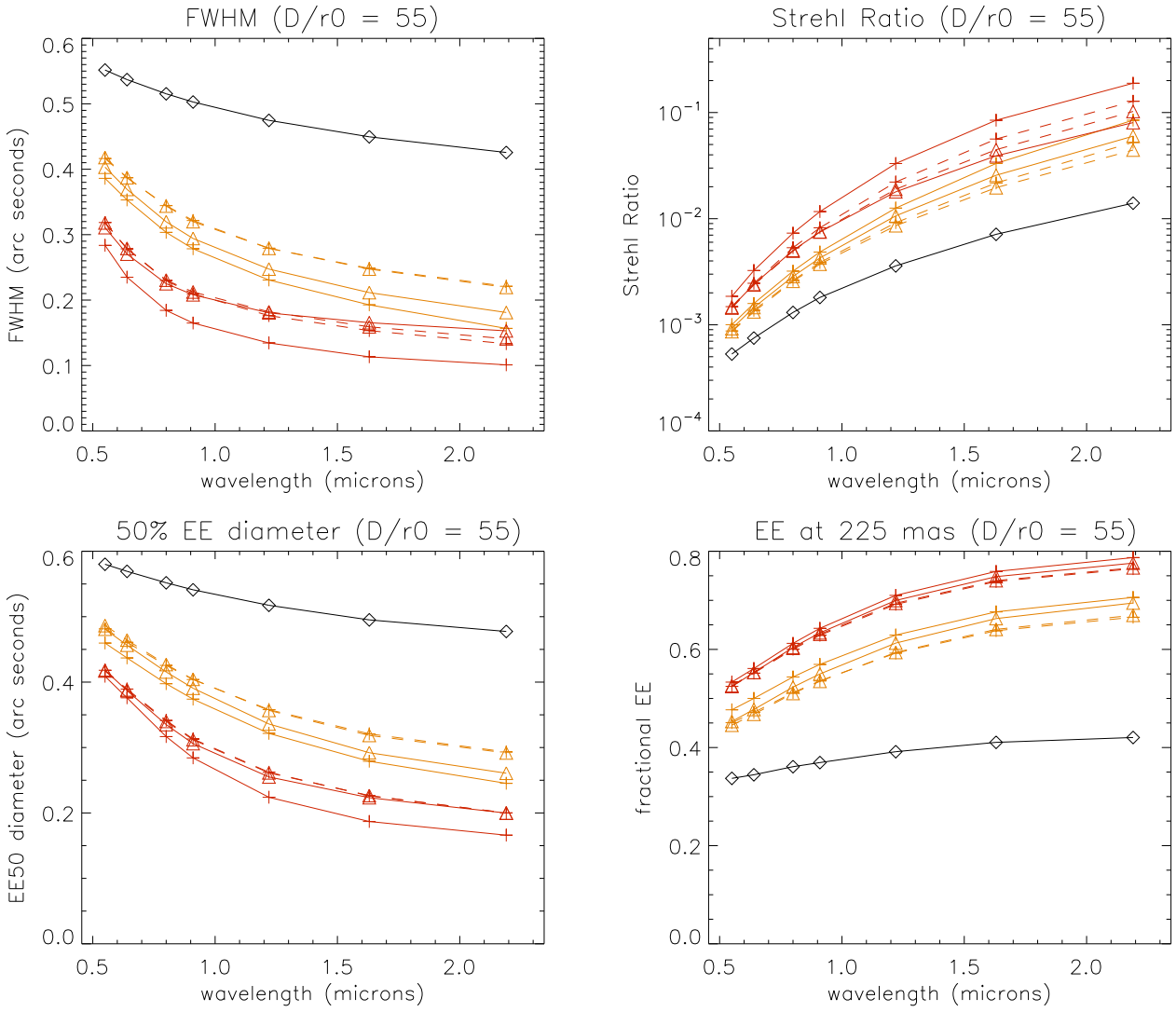

Figure 3: All observing scenarios combined for a given seeing condition: 0.57″. Red curves: 13N; orange curves: CNM3 turbulence profile. Solid lines: 2′ FoV; dashed lines: 5′ FoV. Plus plotting symbol: 1 NGS; diamond plotting symbol: 4 NGS.

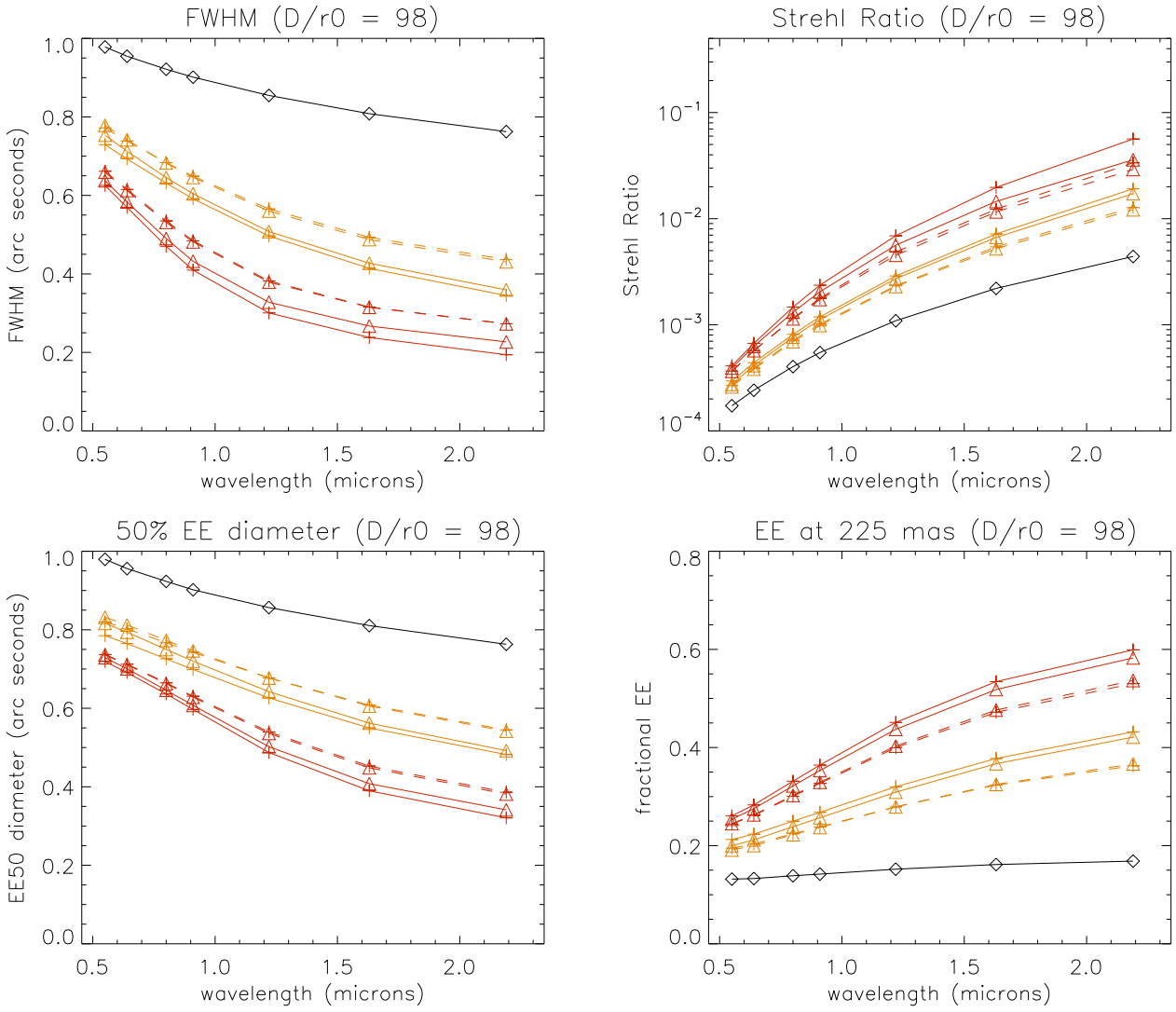

Figure 4: All observing scenarios combined for a given seeing condition: 1.0″. Red curves: 13N; orange curves: CNM3 turbulence profile. Solid lines: 2′ FoV; dashed lines: 5′ FoV. Plus plotting symbol: 1 NGS; diamond plotting symbol: 4 NGS.

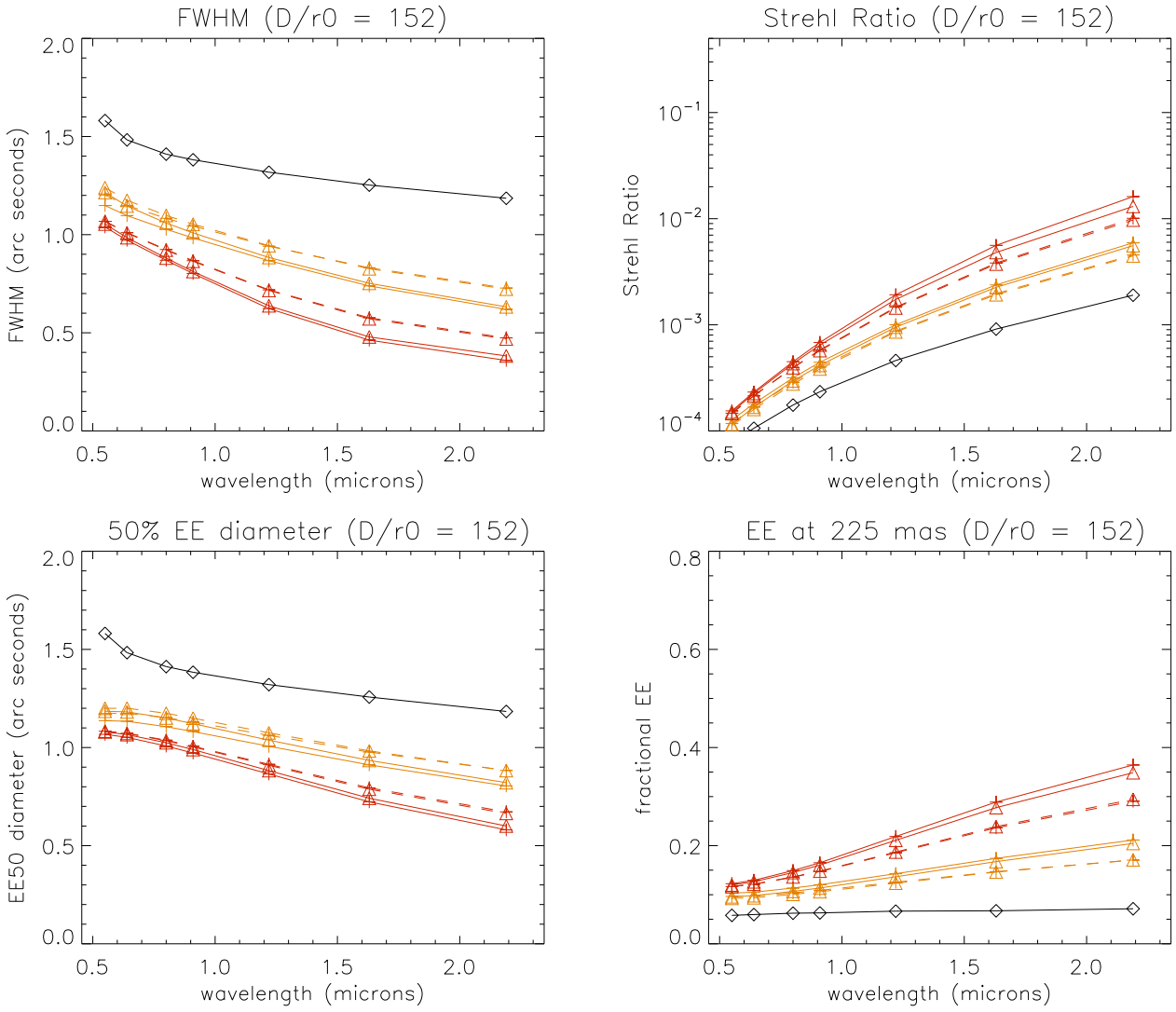

Figure 5: All observing scenarios combined for a given seeing condition: 1.57″. Red curves: 13N; orange curves: CNM3 turbulence profile. Solid lines: 2′ FoV; dashed lines: 5′ FoV. Plus plotting symbol: 1 NGS; diamond plotting symbol: 4 NGS.

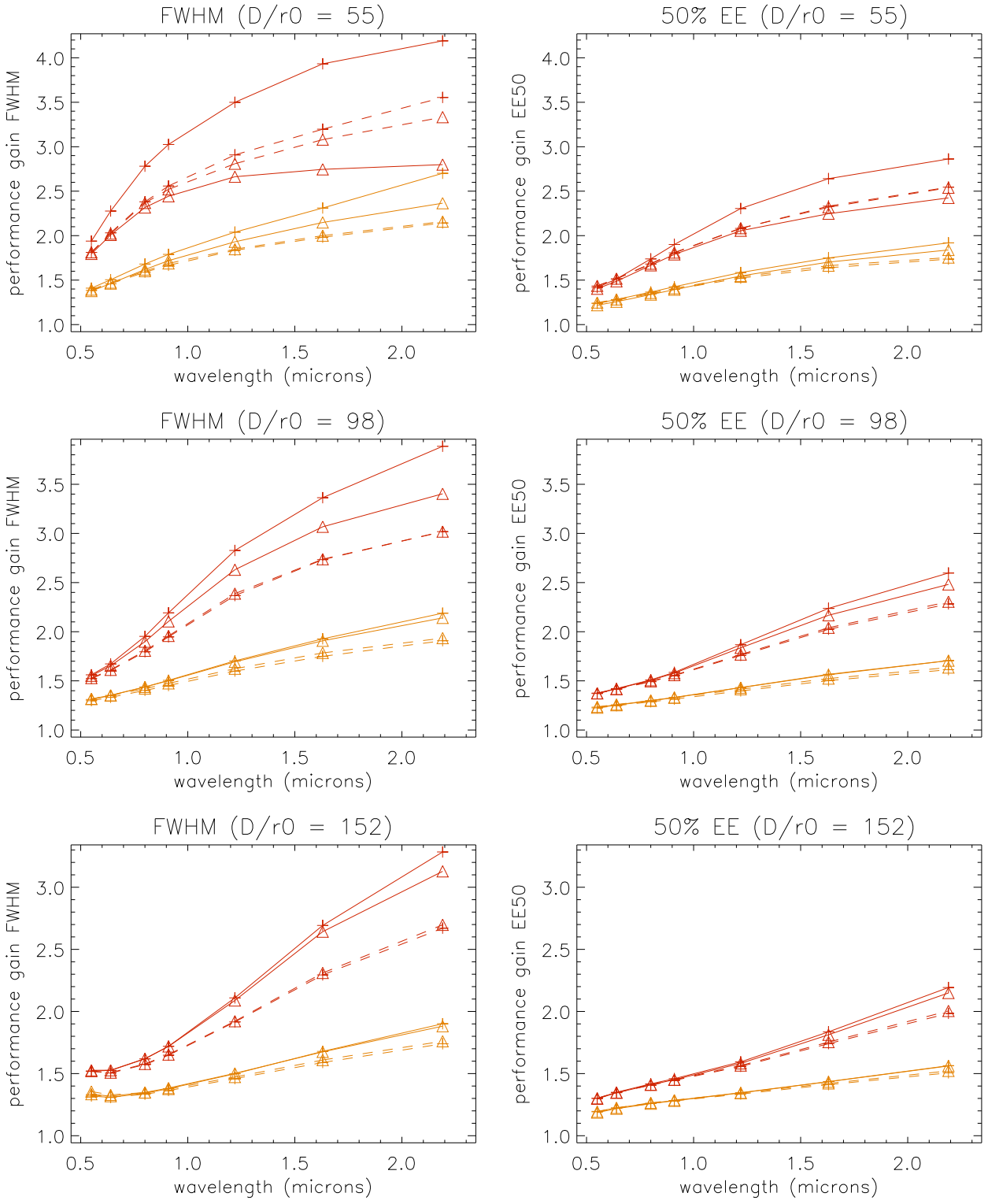

Figure 6: GLAO performance "gain" as defined in text, for a seeing of 0.57″ (top), 1.0″ (middle) and 1.57″ (bottom). Coding same as in previous figures, i.e. red curves: 13N; orange curves: CNM3 turbulence profile. Solid lines: 2′ FoV; dashed lines: 5′ FoV. Plus plotting symbol: 1 NGS; diamond plotting symbol: 4 NGS. See text under Sect. 4 for details.